

A benchmark of different starting modes of a passive Fuel Cell/Ultracapacitor hybrid source for an electric vehicle application

Andres Jacome^a, Clément Dépature^b, Loïc Boulon^b, Javier Solano^a

^a*Grupo de investigación GISEL Universidad Industrial de Santander, Bucaramanga, Colombia*

^b*Institut de Recherche sur l'Hydrogène, Université du Québec à Trois-Rivières, Canada*

Abstract

A benchmark of different starting modes of a passive Fuel Cell (FC) / Ultracapacitors (UCs) hybrid source is presented. Passive hybridization consist to directly connect the FC and the UC without power electronics. Compared with active sources, passive hybridization presents some advantages: lower volume and weight, ease of implementation, and lower cost. However, the power distribution among the sources is no longer controllable. Additionally, the FC-UC passive hybrid source's start-up could lead to high inrush currents and faster FC degradation. A FC-UC passive hybrid source start-up is evaluated by simulations and experimentally. Three starting modes for an automobile application are considered: progressive starting, short circuit, and using a resistive pre-charge device.

Keywords: PEM Fuel cell, passive hybrid source, ultracapacitors, starting operation modes, vehicular application, experimental validation.

1. Introduction

Fuel Cells (FC) are an attractive energy source because of its high energy density, high efficiency, and zero local emissions. However, FC present a limitation on its dynamic response and cannot recover energy, e.g., regenerative braking in vehicular application [31, 6, 44]. Ultracapacitors (UCs) could be a complementary source to lower power density such as FC or batteries due to their fast dynamic, high power density, charge/discharge abilities, and reversibility [35, 7, 30].

FC and UC can be connected using either passive or active configurations [25]. Active configurations use at least one DC/DC converter to couple the FC to the UC. These configurations allow designing and performing a stable control associated with an energy management strategy [17]. However, using additional power converters

generally increases the energy losses, the volume, the weight, and the cost of the hybrid source. Other disadvantages of active configurations are the ripple currents generated by the power converters, which can reduce the lifespan of the FC stack [39].

In a passive connection, FC and UC or FC and batteries [29] are directly connected in parallel without a power converter. Therefore, this configuration does not permit to define a control strategy to determine the power distribution of the hybrid source. The power distribution between FC and UCs depends on the sizing of the system. Passive configuration offers a simple solution at a low cost to eliminate power converters' losses and then increase the system's global efficiency.

Some studies compare the active and passive architecture of a hybrid source composed of a FC system and a batteries or UCs bank as an auxiliary power source for transport applications. Samsun et al. [32] consider a FC and batteries hybrid system for truck applications. The study shows that the passive connection has a better performance during short-time load variations. However, long fluctuations presented by the load could cause that the FC works in low-efficiency regions. Xun et al. [43] use a FC system combined with Li-ion batteries or ultracapacitors to power an electrical vehicle. The results demonstrate that the FC/UCs passive hybridization presents a better performance than the FC/batteries active configuration in terms of FC assistance, *i.e.*, as UCs have a better state of charge (SoC) level during the used driving cycle than batteries, Ultracapacitors easily capture the high power demand avoiding the FC performance degradation. In [41] the evaluation of a fuel cell and ultracapacitors direct connection under an automotive profile reveals that UCs can reduce the high current demand of the FC and its dynamic current value when a variable cycling is applied. This is due that UCs have a low impedance and then they work as a low-pass filter removing all the high current peaks which are addressed to FC. Macias et al. [25] presents a comparison between the FC/UCs passive and active architecture subjected under an automotive load cycling. Simulation results show that the passive coupling presents 17% less of hourly operation cost. This operation cost includes, for instance, the hydrogen consumption and the capital cost of the sources. Considering an automobile cycling, which normally imposes certain hard operation conditions such as high current demand in short time [22], and based on these previous manuscripts, the selection of a passive architecture of a fuel cell and a ultracapacitors bank seems to be the best choice.

Recent researches have studied the passive configuration of FC and UCs. Garcia et al. [20] analyze the effect of sizing these energy sources on the power distribution. Depature et al. [18] proposes a sizing methodology based on three criteria: UCs storage capacity, UCs maximal voltage, and the FC operation current dynamic,

allowing the FC to meet the load requirements, extend its lifetime, and improve its global efficiency. Zhao et al. [45] make a study by simulation of different powertrain configurations of FC/UC hybridization. Results show that the passive configuration presents the lowest hydrogen consumption due to the losses elimination at the DC/DC converters. Ait Hammou Taleb et al. [2] shows in an experimental research that, connecting all cells of a FC stack individually to low relatively capacity UC may be a convenient way to homogenize their voltage evolution during transients. Morin et al. [28] study the FC/UC passive connection at the scale of each cell of a FC stack. Silva et al. [34] analyze the FC/UC direct connection by simulation and experimentally study the effect of the high current during the connection, on the FC degradation. Turpin et al. [38] presents a passive connection at the cell scale, *i.e.*, each fuel cell of the stack is directly connected in parallel with an elementary ultracapacitor. Authors declare that the passive connection protects the FC against high peak currents and the harmonics current produced by the power converters. Arora et al. [4] hybridize a single fuel cell with one or three 3000F UCs. Increasing the number of UCs, the FC decreases its hydrogen consumption per cycle by around 5%. Therefore, an improvement of the FC and the hybrid source performance by 10% and 16% respectively is presented.

Another advantage of hybridization of FC and UC is that this configuration reduces the occurrence of flooding in the FC and the degradation of the FC. This is because the water production in the FC is linked to the FC current, which is smoothed by the presence of UC [3, 5]. Moreover, by increasing the UCs capacity, the FC is less demanded during load variation periods. Similar conclusions are given in [42], UCs protect the FC from high current peaks because of their lower impedance. In this case, UCs act as a low-pass filter. Therefore, FC could extend its lifetime as it is required only to supply the average load power. Based on the previous works, passive architecture seems particularly attractive for an FC/UCs hybridization in terms of: system cost, FC lifetime protecting and FC performance increasing. However, a challenge that is not yet explored for this architecture and deserves to be tackled is the starting phase.

The starting phase of a UCs/FC passive hybrid source is a critical point since UCs voltage can be lower than FC one or UCs can be discharged because of its self-discharge phenomenon (UC losses between 5-15% its initial voltage within 48h after full charge [23]). In this case, FC could be connected in parallel with a discharged source; therefore, the FC will operate in a short circuit. This short circuit condition causes high inrush currents, which could affect the FC lifespan [22]. Hinaje et al. [21] connect a single FC with a discharged UC and propose to control the current by mass transfer losses and the hydrogen flow. Silva et al. [34] operate the FC in a

short circuit, they turn on the FC and then the stack is directly connected with the discharged UC bank. Besides, the authors suggest, as a future work, a progressive starting using a real PEMFC stack, i.e., connect the FC with UC and then turn on the FC to progressively charge the UC. Wu et al. [40] use a fixed resistor to charge the UCs to just below the FC open-circuit voltage (OCV). These starting methods mitigate the problem of high peak currents during the start phase. However, few papers present experimental results on the start-up of an FC/UC hybrid source. The majority of them have studied this issue at fuel cells scale, i.e., not using a commercial stack and considering unrealistic load profiles. This paper contributes to the study by simulating and experimenting with the starting phase of an FC/UCs passive source under a real automotive load cycle and considering commercial components.

This paper aims to model, simulate, and experimentally evaluate a passive hybrid source composed of a Horizon Proton Exchange Membrane (PEM) FC and Maxwell UC. Three different start modes are evaluated: short-circuit, progressive, and using a resistive precharge device. Therefore, the paper is organized as follows: Section II presents the model of each component of the system and the Energetic Macroscopic Representation (EMR) to integrate them. Section III presents a sizing methodology and its application to the hybrid source. Section IV presents the three different start modes of the passive hybrid source, and the experimental validation is shown in Section V. Section VI presents the conclusions.

2. Modeling and energetic macroscopic representation

The hybrid source is composed of a PEMFC and UCs. They are coupled using a diode to prevent currents flowing from the UC to the FC. This hybrid source is connected to a traction subsystem (TS) corresponding to an electric vehicle. The traction subsystem includes a voltage-source converter (VSC), a three-phase induction machine, a gearbox, a differential, and the wheels. All the traction subsystem is modeled as an equivalent current source, which acts as an electric load. Figure 1 shows the studied architecture of the FC/UCs direct hybrid source.

2.1. Modeling

UCs are modeled using the Zubieta circuital model[46]. This circuital model is composed of two branches, as illustrated in Figure 2, the principal branch represents the internal resistance R_i and the energy accumulation by considering a constant capacitor C_{i0} and a non-linear capacitor $C_{i1}V_{eq}$. The secondary branch models the self-discharge phenomenon by considering a resistance R_2 and the charge redistribution by considering a constant capacitor C_2 .

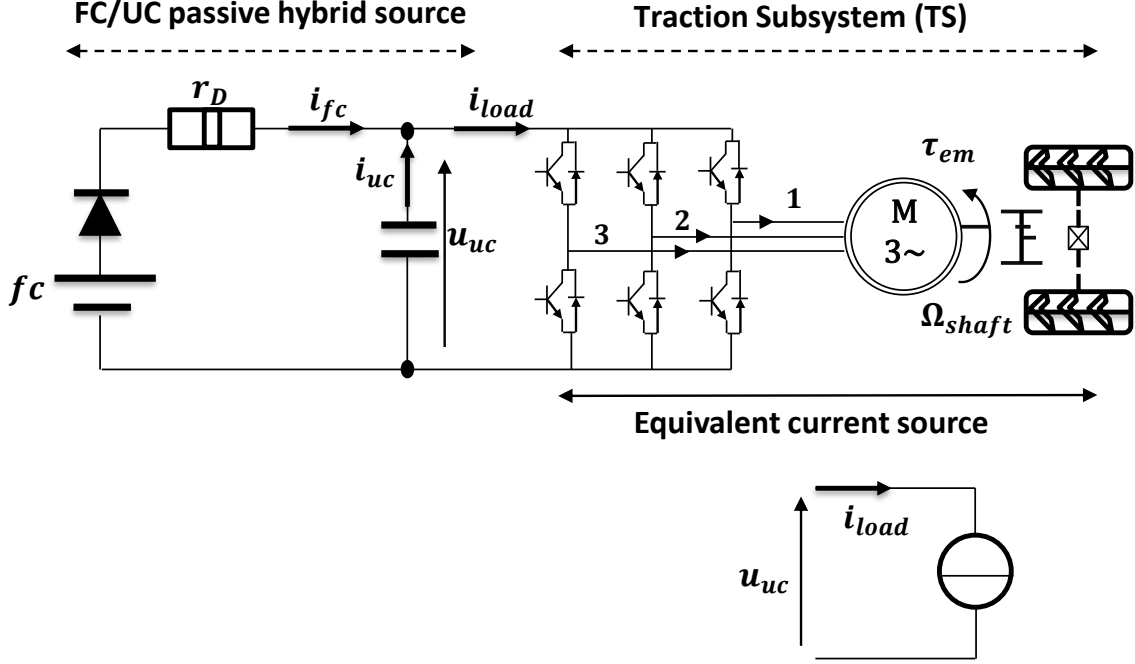


Figure 1: FC/UC passive hybrid source architecture

The FC model and parameters presented in [10] are selected. The PEMFC system model is divided into three submodels: the electrochemistry, the thermal, and the fluidic (air and hydrogen supply) model. The equations which represent the model are presented in Table 1 and Table 2.

The diode resistance/losses are modeled using an equivalent constant resistance r_D as:

$$\frac{u_{fc} - u_{uc}}{r_D} = i_{fc} \quad (18)$$

with u_{fc} and u_{uc} the FC stack and the UCs voltage, respectively, and i_{fc} the FC current.

The sources and the load are coupled via a DC bus. The UC impose their voltage u_{uc} to the bus while the FC/diode subsystem operates as a current source. The current of the load i_{load} is equal to the sum of the FC and UC currents, i_{fc} and i_{uc} as defined by Equation 19. The FC/SC passive connection is modeled using the Kirchoff's current law:

$$i_{fc} + i_{uc} = i_{load} \quad (19)$$

2.2. Models integration using the EMR

The Energetic Macroscopic Representation (EMR) is a synthetic graphic tool for systematically analyzing the interactions between subsystems in multi-physics systems. Pictograms represent the elements of a system and are interconnected following two principles: the action-reaction and the integral causality. Moreover, EMR has been used to study multi-physics multi-sources systems [1, 11], photovoltaic generation systems [24], or hybrid electrical vehicles [9]. More detailed information about EMR can be found in [12].

The FC, UC, and the load models are integrated using the EMR formalism, as shown in Figure 3. The FC, the UC, and the load are represented by energy sources (green oval pictograms). The parallel connection between the FC, UCs, and the TS is represented by a mono-domain distribution element (overlapping squares). The diode resistance, connected between the FC/UC parallel connection, imposes the UCs charge current value and is represented as a mono-domain conversion block depicted by an orange square pictogram.

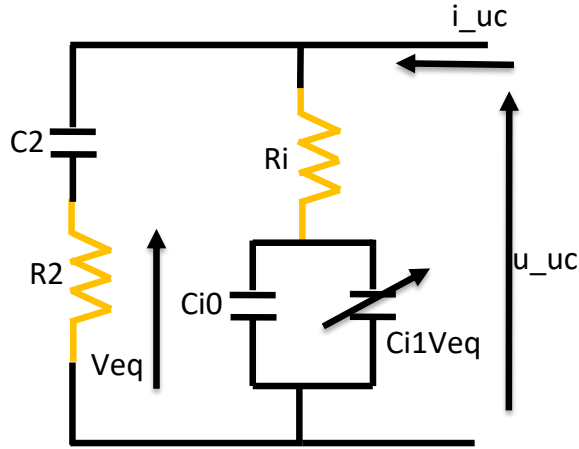


Figure 2: UC equivalent electrical circuit

3. Sizing methodology

A passive hybrid source does not include power converters; therefore, there is no control anymore, and a natural power distribution between the energy sources occurs. This power distribution depends on the internal impedance of the sources [42]. A sizing methodology is required to determine the optimal size of these sources and to have an adequate power distribution. The proposed sizing methodology is based on

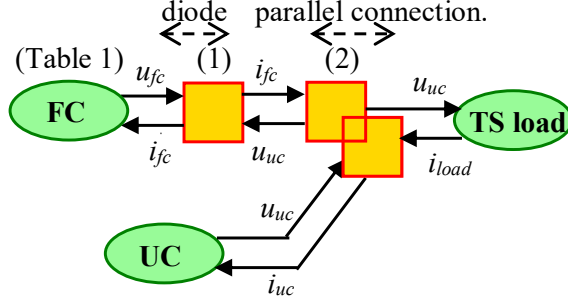


Figure 3: EMR of the studied FC/UC passive connection

our previous research work [19] and is adapted for this case. The sizing methodology uses as inputs a reference power profile and data-sheets from commercial FC and UCs. An exhaustive search algorithm is then used to find all the possible configurations of available FC and UCs supplying the reference power. The simulation results are evaluated, considering the following three criteria:

1. FC is not reversible and has limits on the power magnitude (p_{fc}).
2. The FC current dynamic ($\frac{di_{fc}(t)}{dt}$) supplied cannot be higher than its maximal value ($\frac{di_{fc-max}}{dt}$) because its current dynamic is strongly related to the air dynamic feeding.
3. The UC voltage ($u_{uc}(t)$) can never exceed its maximal value (u_{uc-max}) as UCs should never be overcharged for security reasons.

Potential solutions are rejected if they do not respect these criteria. The accepted solutions performance are evaluated through the objective function presented in (Equation 20) [16, 15, 14, 13]. The objective function considers the hydrogen consumption (C_{H_2}) (Equation 21), which depends principally on the Hydrogen mass flow (\dot{m}) and the fuel cell current (i_{fc}), and the FC degradation cost ($C_{\Delta_{fc}}$) (Equation 23), which depends on the FC turn on/turn off number (N_{switch}), the FC supplied power ($p_{fc}(t)$) and the FC system real cost (FC_{cost}). Equation 22 and Equations 24, 25 are auxiliary ones from Equation 21 and Equation 23 respectively. Considering that the number of UCs life cycles is usually much higher than FC life cycles ones [8], in this paper, the cost of life of UCs is neglected.

$$F_{cost} = C_{H_2} + C_{\Delta_{fc}} \quad (20)$$

$$C_{H_2} = \int_0^t \dot{m}_{H_2} dt H_{2_{cost}} \quad (21)$$

$$\dot{m}_{H_2} = i_{fc} \frac{NM_{H_2}}{2F\lambda} + \dot{m}_{H_2-init} \quad (22)$$

$$C_{\Delta_{fc}} = \Delta_{fc}(t) FC_{cost} \quad (23)$$

$$\Delta_{fc}(t) = \int_0^t \delta(t) dt + N_{switch} \quad (24)$$

$$\delta(t) = \frac{\delta_0}{3600} \left(1 + \frac{\alpha}{p_{fc-nom}^2} (p_{fc}(t) - p_{fc-nom}) \right) \quad (25)$$

Where $H2_{cost}$ is the cost of hydrogen ($\$US/gH_2$), N is the number of cells connected in series inside the FC stack, λ is the FC generating efficiency, M_{H_2} is the molar mass of hydrogen, F is the Faraday constant, δ_0 and α are load coefficients, p_{fc-nom} is the FC nominal power, Δ_{fc} is expressed between 0 (start of life) and 1 (end of life) and $C_{\Delta_{fc}}$ is the FC degradation cost ($\$US$). The lowest cost solution is selected. This methodology, presented and summarized in Figure 4, is used to size a small-scale test bench of UCs to be directly connected to a FC.

3.1. Study case

This subsection presents the proposed sizing methodology application for a particular case. Firstly, the inputs are defined; secondly, the selection criteria are evaluated. Third, the objective function determines the lowest cost solution. Finally, the sized hybrid source is put into operation to evaluate its power distribution given by the sizing algorithm.

3.1.1. Inputs

This paper considers a Horizon 500W PEMFC and a dynamic power profile. The PEMFC has a maximal voltage or open-circuit voltage (OCV) of 31.4V and a maximal current dynamic ($\frac{di_{fc-max}}{dt}$) of 2A/s [36, 37]. The power profile is obtained from collected measurements of a real electric vehicle [26]. This power profile is scaled down to 300W (scale 1/60) to adapt an 8500 programmable electronic load used for experimental validation.

UCs are selected considering the FC OCV and commercial availability from Maxwell[27]. The UCs maximal voltage can not be lower than FC OCV because both sources are connected in parallel. FC can support OCV condition, but if the UCs maximal voltage is below the FC OCV value, UCs will be overcharged. Therefore, the selected UC configurations are 32V 8F (two modules connected in series of 16V and 16F), 32V 29F (two modules connected in series of 58F and 16V) and 32V 58F (four modules of 16V and 58F; two pairs of modules are connected in series, each pair of 32V 29F, and then the two pairs are connected in parallel).

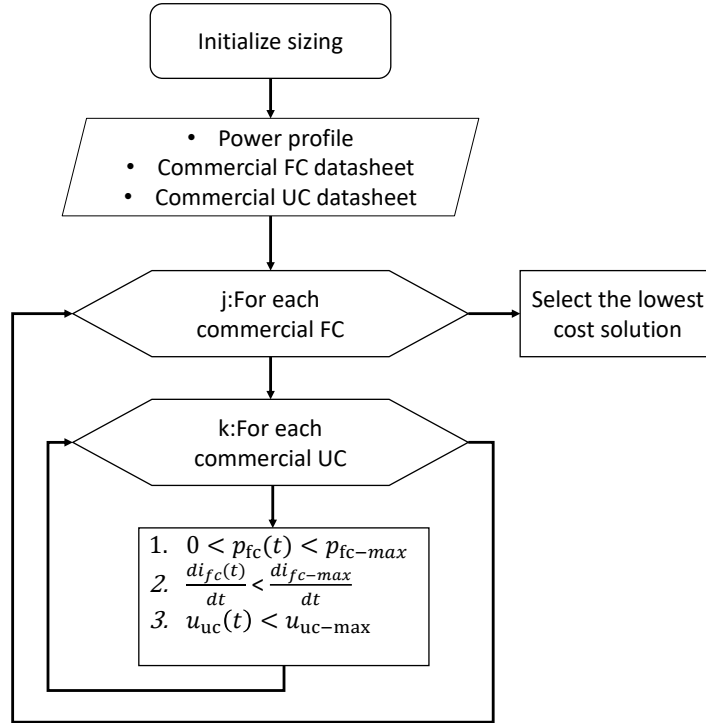


Figure 4: Sizing methodology [19]

3.1.2. Criteria evaluation

The model of the system presented in Section II is implemented in Matlab/Simulink to evaluate the proposed sizing methodology. Moreover, the simulation model parameters are presented in Table 3. The simulation results for each UC configuration with an initial voltage ($u_{uc-init}$) of 30V are presented in Figure 5. They are evaluated based on three criteria: the FC power magnitude, the FC current dynamic, and the UC voltage.

As it can be seen in Figure 5, the 8F UC presents a higher FC current dynamic than its defined maximal dynamic (2 A/s). Moreover, this UC configuration is overcharged at the end of the cycle. Therefore, this solution is rejected. On the other hand, the 29F and 58F configurations are accepted as possible solutions because they respect all the criteria.

3.1.3. Objective function evaluation

The accepted solutions are compared using the objective function presented previously. In Table 4 the costs per cycle of hydrogen consumption and FC degradation

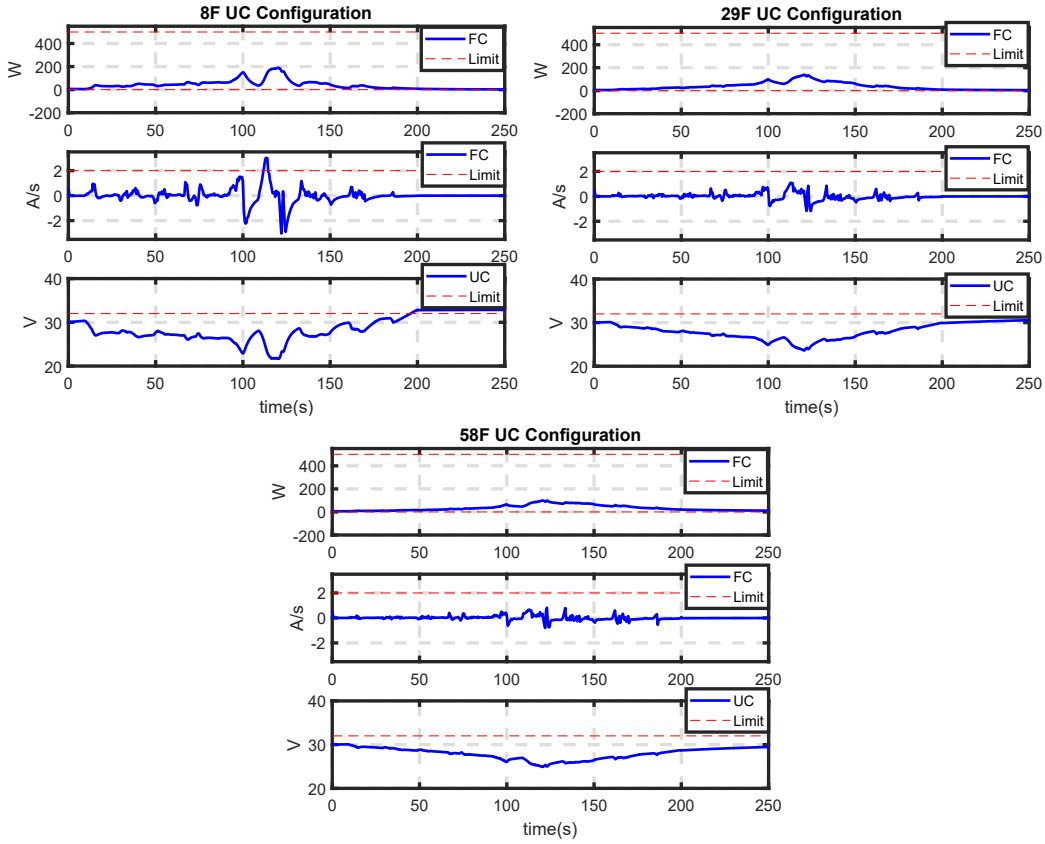


Figure 5: Simulation results for the three UC configurations: 8F UC: power (up), current dynamic (middle) and voltage (down), 29F UC: power (up), current dynamic (middle) and voltage (down), 58F UC: power (up), current dynamic (middle) and voltage (down)

are presented.

The objective function selects the solution, which represents the total lowest cost ($C_{tot}/cycle$). Thus, the 29F UC configuration is considered for experimental validation.

3.1.4. Sized hybrid source evaluation

The hybrid source is evaluated under the reference profile to analyze the energy sources' power distribution. The operation of the system is presented in Figure 6. UCs can assist the FC to supply the power demanded by the load. The FC supply the mean power of the load, and UCs respond to power variations. Besides this, UCs are charged by the FC, when the FC power is higher than the load power, e.g., at 100s.

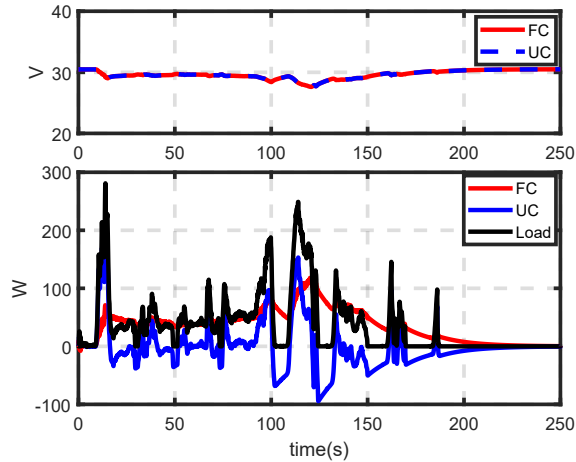


Figure 6: Passive hybrid source operation: voltage (up) and power (down)

4. Starting procedures

The operation of the passive hybrid source presented in Section III shows an adequate power distribution. However, the starting phase is not yet studied. The procedure to start-up the hybrid source needs to be examined because two sources are directly connected in parallel. In this case, UCs impose the voltage to the system. One major inconvenience is that UCs voltage naturally decays, and thus they can be discharged. This inconvenience affects the FC durability because it could be in a short circuit, which causes high inrush currents.

The current of the system (i_{fc}) depends on two factors: the potential difference between FC and UCs and the FC, UCs, and diode resistances (r_D). However, these resistance values are normally low [34]. Therefore, the system will have a high inrush current (i_{fc}) if the FC is connected with discharged UCs (see Equation 18). The most common procedure to reduce this high peak of current during the passive connection is to place a resistor between the sources[40]. This resistor is used to charge the UCs bank, and once the UCs are charged, the resistor is disconnected to have a direct connection. Other alternative procedures like the short circuit and the progressive starting do not consider a resistor to start the passive hybrid source. Progressive starting consists in connecting the UCs and the fuel cell, and then the latter is turned on. In this way, the FC could progressively charge the UCs if the stack is progressively fed with the H_2/O_2 gases [28]. In the short-circuit procedure, firstly, the FC is turned on, and then the stack is connected with the UCs. This procedure uses the phenomenon of mass transfer losses and the hydrogen flow to limit the UCs

charging current [21, 34].

Three starting procedures for the passive FC/UC hybrid source are identified and simulated in this section: the short circuit operation, the progressive starting, and using a fixed resistance (resistive pre-charge device).

4.1. Resistive pre-charge device

A fixed resistance of 1Ω is selected to charge the UCs up to the FC OCV. Simulation results are presented in Figure 7. The FC current is reduced to 14.89A (approximately two times its nominal value, 30A), but the UCs are charged in approximately 200s.

4.2. Short circuit starting

The short circuit operation consists of turning on the FC, and then the stack is connected with the discharged UCs. This procedure is simulated, and the results are presented in Figure 8. During the connection, the FC current i_{fc} reaches a value of 100A, but only for 300ms, then it drops instantly to 40.35A, and finally, the FC current drops to 0A. Regards the hybrid source voltage, the voltage increase progressively and rapidly the UCs are charged in around 50s due to this transitory peak of current.

4.3. Progressive starting

The progressive starting consists of connecting the FC with the discharged UCs before the FC is turned on. Simulation results are presented in Figure 9. Like the previous method, this third starting method presents a high peak of current in a short time (less than 300ms), then it drops instantly to 34.92A, and finally, it reduces to 0A. As in the short circuit operation, the hybrid source voltage increases progressively, and the UCs are charged at 50s.

4.4. Discussion

Table 5 compares the performance by simulation of the three proposed starting modes. The first method uses a resistive device, allows controlling the charging current to gradually charge the UCs and avoid high peaks of current during the passive connection. However, the method requires more time than progressive and short circuit modes to charge the UCs. Progressive and short-circuit modes present different steps to proceed, but, their results in terms of UC state-of-charge and FC charging current are practically similar. Besides, simulation results show that a high peak of current occurs during the connection in both procedure modes, this high inrush current depends on the SoC level of UCs, results show that this current value decreases at the same time that the charge level of UCs increases. Once the UC are fully charged the FC current is stabilized to 0A.

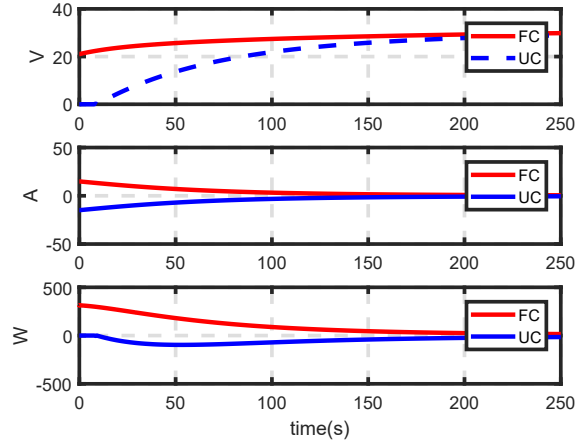


Figure 7: Using a fixed resistance: voltage (up), current (middle) and power (down)

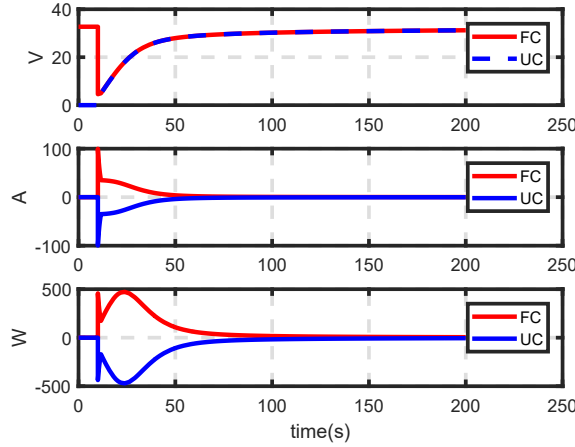


Figure 8: Short circuit starting: voltage (up), current (middle) and power (down)

5. Experimental validation

A hardware-in-the-loop (HIL) test bench is developed at the UQTR Hydrogen Research Institute (HRI) to validate the passive FC/UC hybrid source's starting procedures previously presented. The wiring diagram and the test bench are showed in Figure 10 and Figure 11, respectively. The test bench comprises a H-500 FC stack of 36 cells connected in series from manufacturer Horizon (Nominal characteristics: 16.6V at 30A for 500W), two ultracapacitors modules of nominal values 58F-16V are connected in series from manufacturer Maxwell, whose equivalent UC nominal values are 32V-29F. A 300W programmable DC electronic load is used to reproduce

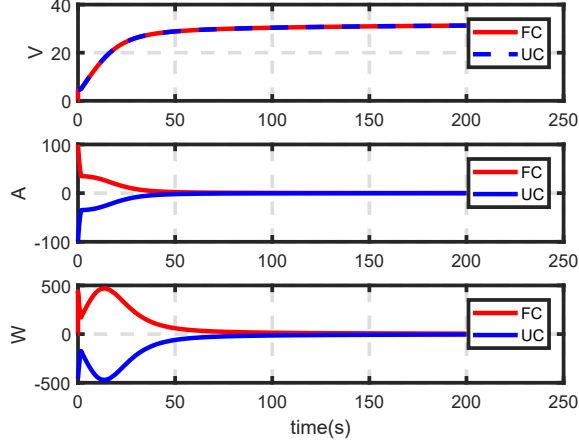


Figure 9: Progressive starting: voltage (up), current (middle) and power (down)

the reduced scale power profile. The programmable DC load is then chosen as a load drive with a power reduction of 60 compared to the full-scale studied vehicle. Besides, the regenerative braking phases are not considered because the programmable load only provides positive power. Only mechanical braking is considered for the braking phases. The FC, the UC, and the programmable load are connected through four contactors K1, K2, K3, and K4, respectively. They provided electrical isolation for each component. A NI 6229 controller operates all the contactors through an designed electronic card and an application developed in LabView. In line with the FC, ultracapacitors, and generator load device, a fuse provides additional passive protection in the case of large in-rush currents. A diode in series with the PEMFC prevents current flowing from the UCs to the FC. This misoperation could happen if the PEMFC voltage drops below that of the UCs. Moreover, a fixed resistance of 1Ω is used for the resistive precharge procedure.

5.1. Resistive pre-charge device

In this procedure an additional contactor (K2) is added in order to connect the resistance during the start-up and disconnect it during the direct connection. To start the experimental procedure, firstly the H_2 and O_2 reactant gases are introduced to the stack, then the contactor K2 is opened, and contactors K1 and K3 are closed. The procedure is validated, and the experimental results are illustrated in Figure 12. This procedure clearly allows us to: avoid exceeding the FC nominal current value observed in the simulation results for the short-circuit and progressive procedure and limit the charge current (i_{fc}) for the UCs. Therefore, the FC current (i_{fc}) is

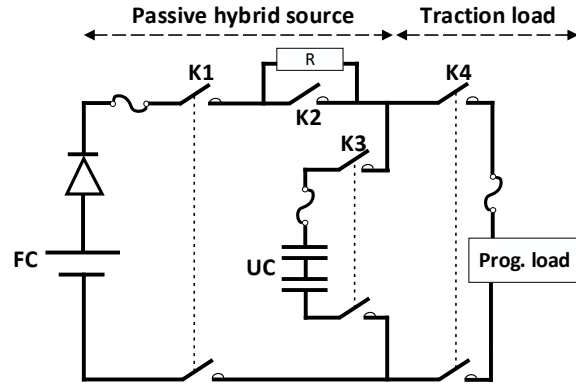


Figure 10: Test bench wiring diagram

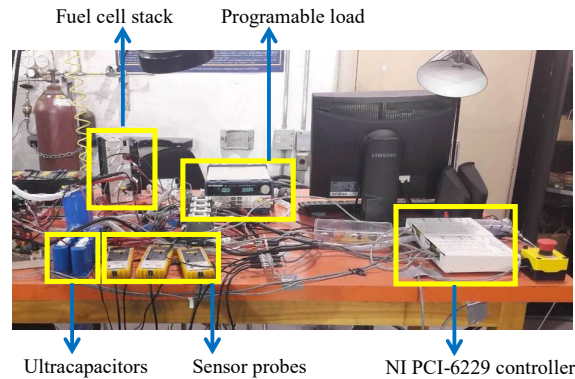


Figure 11: Test bench

reduced to 21.57A, but the time to charge the UCs bank is increased (200s), similar to simulation results.

5.2. Short circuit starting

Short circuit operation turns on the FC and then closes contactors K1, K2, and K3 to connect the FC with the UCs. Experimental results are presented in Figure 13. Like presented in the previous section, simulation results, the hybrid source increases its voltage progressively until the UCs are charged after 50s. Differently from simulation results, the FC presents three high inrush currents instead of one peak, the first one of 66A; then, it is reduced to 38.36A, which corresponds to the stoichiometric H_2 flow rate [21], and stabilized to 0A. The two other ones, the high inrush currents are decreased as soon as the UCs bank are charged. Again, compared to the precedent section, this phenomenon is not appreciated in simulation, the

PEMFC is disconnected three times by the commercial controller. This disconnection is because the stack reaches its maximal current value (42A). Therefore, the PEMFC requires at least this number of times (3) to be turned on for charging the UCs.

5.3. Progressive starting

The progressive starting closes contactors K1, K2, and K3, and then, the FC is turned on. Experimental results are illustrated in Figure 14. Similar to simulation results, the hybrid source progressively increases its voltage until the UCs are charged during approximately 50s. The three transitory high peaks of current occurred during the connection are reduced because the mass transfer losses and the H_2 flow, quite similar as the short circuit starting. However, with a real FC, the stack is automatically disconnected by the FC controller and it has to switch on three times to finalize the UCs charge. This phenomenon is not visualized by Hinaje et al. [21] principally because they consider on their study a single fuel cell, not a commercial PEMFC stack.

5.4. Discussion

The proposed starting modes are experimentally validated, and the results are summarized in Table 6. The time of UCs charging is quite similar compared to simulation results for the three modes. However, the reached maximal instantaneous current by the PEMFC stack corresponds to approximately two times its nominal value (30A) using the progressive and the short circuit procedures. These experimental results are different from the simulation results. This difference can be explained by the fact that the PEMFC controller is not modeled in the simulation model. Therefore, the simulation model can not describe the instants where the PEMFC is disconnected three times by the controller because its limit current (42A) is exceeded. Although a short demand (few milliseconds) of high current density could improve the FC performance as it can remove the oxygenated species from the Electrode platinum (Pt) active surface [34], the fact of switch on/off automatically the fuel cell three times to finalize the UCs charge and repetitively exceeding the FC maximal current could affect the thermal behaviour of the system [16]. In this case, the produced water due to the normal electro-chemical reaction will not be enough to keep correctly humidified the FC membrane and then the stack lifespan will be impacted. Concerning the comparison of the resistive pre-charging mode between the experimental and simulation results, both are quite close. This method presents certain shortcomings such as: one additional contactor needs to be added (K2) to the configuration, the dissipated energy due to the resistance could be stored by the UCs and the time to charge the UCs is longer (200s compared to 50s) than the other

mentioned procedures. However, this solution masters better the charging current for UCs and offers protection to the FC against high inrush current presented during the direct connection. Based on this, we consider that this approach seems to be the most adequate mode to start-up the hybrid source. The same conclusion was patented by NISSAN Motor co. [33].

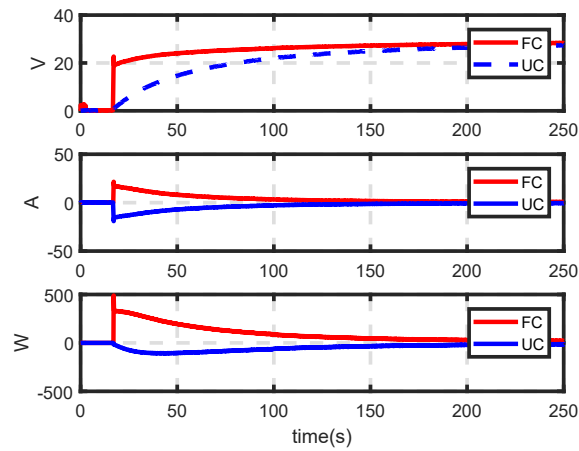


Figure 12: Resistive precharge device-Experimental results: voltage (up), current (middle) and power (down)

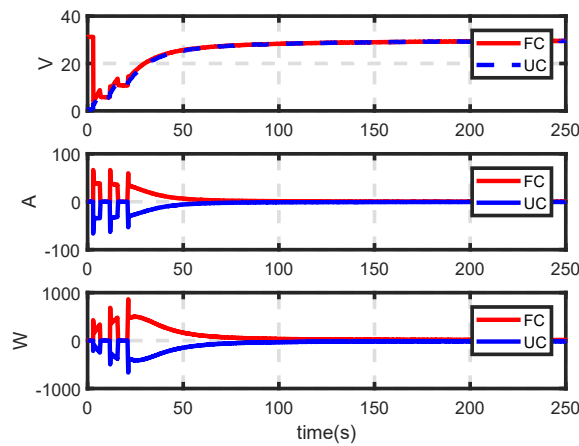


Figure 13: Short circuit starting-Experimental results: voltage (up), current (middle) and power (down)

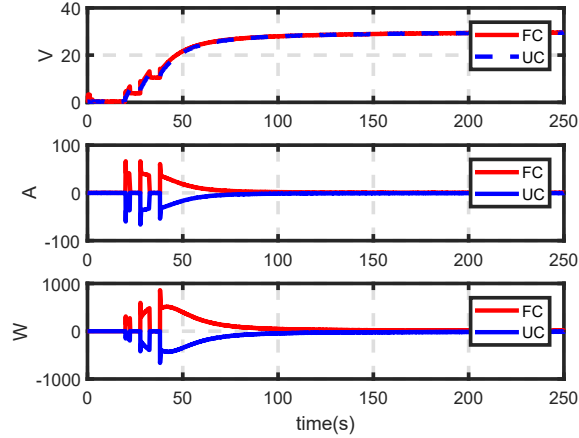


Figure 14: Progressive starting-Experimental results: voltage (up), current (middle) and power (down)

6. Conclusion

This paper presented a benchmark of three starting modes of a passive FC/UC hybrid source. The pre-charge (using a resistance), short circuit, and progressive procedures are identified and compared by simulation and experimental results. Short circuit and progressive starting modes use different steps. However, their results are quite similar in terms of UCs voltage and FC current. Both procedures have the shortcoming of presenting high inrush currents during the passive connection causing an automatic disconnection of the FC by the controller. Although the pre-charge concept (using a fixed resistance of 1Ω) requires more time to charge UCs, this method seems to be the most adequate to start-up the passive hybrid source. This procedure can limit the FC degradation by reducing the inrush currents during the direct connection.

References

- [1] KS Agbli, MC Péra, D Hissel, O Rallières, C Turpin, and I Doumbia. Multi-physics simulation of a pem electrolyser: Energetic macroscopic representation approach. *International journal of hydrogen energy*, 36(2):1382–1398, 2011.
- [2] S. Ait Hammou Taleb, D. Brown, J. Dillet, P. Guillemet, J. Mainka, O. Crosnier, C. Douard, L. Athouël, T. Brousse, and O. Lottin. Direct Hybridization of Polymer Exchange Membrane Surface Fuel Cell with Small Aqueous Supercapacitors. *Fuel Cells*, 18(3):299–305, 2018.

- [3] D. Arora, C. Bonnet, M. Mukherjee, S. Arunthanayothin, A. Shirsath, M. Lundgren, M. Burkardt, S. Kmiołek, S. Raël, F. Lopicque, and S. Guichard. Long term study of directly hybridized proton exchange membrane fuel cell and supercapacitors for transport applications with lower hydrogen losses. *Journal of Energy Storage*, 28(February):101205, 2020.
- [4] D. Arora, K. Gérardin, S. Raël, C. Bonnet, and F. Lopicque. Effect of supercapacitors directly hybridized with PEMFC on the component contribution and the performance of the system. *Journal of Applied Electrochemistry*, 48(6):691–699, 2018.
- [5] Divyesh Arora, Caroline Bonnet, Mainak Mukherjee, Stéphane Raël, and François Lopicque. Direct hybridization of PEMFC and supercapacitors: Effect of excess hydrogen on a single cell fuel cell durability and its feasibility on fuel cell stack. *Electrochimica Acta*, 310:213–220, 2019.
- [6] E. Maximiliano Asensio, Guillermo A. Magallán, Cristian H. De Angelo, and Federico M. Serra. Energy Management on Battery/Ultracapacitor Hybrid Energy Storage System based on Adjustable Bandwidth Filter and Sliding-mode Control. *Journal of Energy Storage*, 30(December 2019):101569, 2020.
- [7] Simone Barcellona, Luigi Piegari, and Andrea Villa. Passive hybrid energy storage system for electric vehicles at very low temperatures. *Journal of Energy Storage*, 25(June):100833, 2019.
- [8] Jennifer Bauman and Mehrdad Kazerani. A comparative study of fuel-cell–battery, fuel-cell–ultracapacitor, and fuel-cell–battery–ultracapacitor vehicles. *IEEE Transactions on Vehicular Technology*, 57(2):760–769, 2008.
- [9] D Bienaimé, N Devillers, MC Péra, F Gustin, A Berthon, and ML Grojo. Energetic macroscopic representation as an efficient tool for energy management in a hybrid electrical system embedded in a helicopter. In *Electrical Systems for Aircraft, Railway and Ship Propulsion (ESARS), 2012*, pages 1–6. IEEE, 2012.
- [10] L Boulon, K Agbossou, D Hissel, P Sicard, A Bouscayrol, and M-C Péra. A macroscopic pem fuel cell model including water phenomena for vehicle simulation. *Renewable energy*, 46:81–91, 2012.
- [11] A Bouscayrol, P Delarue, X Guillaud, W Lhomme, and B Lemaire-Semail. Simulation of a wind energy conversion system using energetic macroscopic representation. In *Power Electronics and Motion Control Conference (EPE/PEMC), 2012 15th International*, pages DS3e–8. IEEE, 2012.

- [12] Alain Bouscayrol, Jean-Paul Hautier, and Betty Lemaire-Semail. Graphic formalisms for the control of multi-physical energetic systems: Cog and emr. *Systemic design methodologies for electrical energy systems: analysis, synthesis and management*, pages 89–124, 2012.
- [13] John Cardozo, Neigel Marx, Loic Boulon, and Daniel Hissel. Comparison of multi-stack fuel cell system architectures for residential power generation applications including electrical vehicle charging. In *Vehicle Power and Propulsion Conference (VPPC), 2015 IEEE*, pages 1–6. IEEE, 2015.
- [14] Huicui Chen, Pucheng Pei, and Mancun Song. Lifetime prediction and the economic lifetime of proton exchange membrane fuel cells. *Applied Energy*, 142:154–163, 2015.
- [15] Clément Dépature. *Commandes par inversion d’un véhicule à pile à combustible et supercondensateurs*. PhD thesis, Université du Québec à Trois-Rivières, 2017.
- [16] Clement Depature, Samir Jemei, Loic Boulon, Alain Bouscayrol, Neigel Marx, Simon Morando, and Ali Castaings. Ieee vts motor vehicles challenge 2017-energy management of a fuel cell/battery vehicle. In *Vehicle Power and Propulsion Conference (VPPC), 2016 IEEE*, pages 1–6. IEEE, 2016.
- [17] Clément Dépature, Walter Lhomme, Pierre Sicard, Alain Bouscayrol, and Loïc Boulon. Real-time backstepping control for fuel cell vehicle using supercapacitors. *IEEE Transactions on Vehicular Technology*, 67(1):306–314, 2018.
- [18] Clément Dépature, Alvaro Macías, Andres Jácome, Loïc Boulon, Javier Solano, and João P. Trovão. Fuel cell/supercapacitor passive configuration sizing approach for vehicular applications. *International Journal of Hydrogen Energy*, may 2020.
- [19] Ricardo Dominguez, Javier Solano, and Andres Jacome. Sizing of fuel cell-ultracapacitors hybrid electric vehicles based on the energy management strategy. In *2018 IEEE Vehicle Power and Propulsion Conference (VPPC)*, pages 1–5. IEEE, 2018.
- [20] Marcos Garcia Arregui. *Theoretical study of a power generation unit based on the hybridization of a fuel cell stack and ultra capacitors*. PhD thesis, INSTITUT NATIONAL POLYTECHNIQUE DE TOULOUSE, 2007.

- [21] M Hinaje, S Raël, J-P Caron, and B Davat. An innovating application of pem fuel cell: Current source controlled by hydrogen supply. *International Journal of Hydrogen Energy*, 37(17):12481–12488, 2012.
- [22] Andres Jacome, Daniel Hissel, Vincent Heiries, Mathias Gerard, and Sebastien Rosini. A review of model-based prognostic for proton exchange membrane fuel cell under automotive load cycling. In *2019 IEEE Vehicle Power and Propulsion Conference (VPPC)*. IEEE, oct 2019.
- [23] Maximilian Kaus, Julia Kowal, and Dirk Uwe Sauer. Modelling the effects of charge redistribution during self-discharge of supercapacitors. *Electrochimica Acta*, 55(25):7516–7523, oct 2010.
- [24] Walter Lhomme, Philippe Delarue, Frédéric Giraud, Betty Lemaire-Semail, and Alain Bouscayrol. Simulation of a photovoltaic conversion system using energetic macroscopic representation. In *Power Electronics and Motion Control Conference (EPE/PEMC), 2012 15th International*, pages DS3e–7. IEEE, 2012.
- [25] A. Macías, M. Kandidayeni, L. Boulon, and J. Trovão. Passive and active coupling comparison of fuel cell and supercapacitor for a three-wheel electric vehicle. *Fuel Cells*, oct 2019.
- [26] Neigel Marx, David Camilo Toquica Cárdenas, Loïc Boulon, Frédéric Gustin, and Daniel Hissel. Degraded mode operation of multi-stack fuel cell systems. *IET Electrical Systems in Transportation*, 6(1):3–11, 2016.
- [27] Maxwell. Product comparison matrix. *Product information*, 2018.
- [28] B Morin, D Van Laethem, C Turpin, O Rallières, S Astier, A Jaafar, O Verdu, M Plantevin, and V Chaudron. Direct hybridization fuel cell–ultracapacitors. *Fuel Cells*, 14(3):500–507, 2014.
- [29] Akira Nishizawa, Josef Kallo, Olivier Garrot, and Jörg Weiss-Ungethüm. Fuel cell and li-ion battery direct hybridization system for aircraft applications. *Journal of Power Sources*, 222:294–300, 2013.
- [30] Poonam, Kriti Sharma, Anmol Arora, and S. K. Tripathi. Review of supercapacitors: Materials and devices. *Journal of Energy Storage*, 21(October 2018):801–825, 2019.

- [31] Aqeel Ur Rahman, Iftikhar Ahmad, and Ali Shafiq Malik. Variable structure-based control of fuel cell-supercapacitor-battery based hybrid electric vehicle. *Journal of Energy Storage*, 29(February):101365, 2020.
- [32] Remzi Can Samsun, Carsten Krupp, Sidney Baltzer, Bruno Gnörich, Ralf Peters, and Detlef Stolten. A battery-fuel cell hybrid auxiliary power unit for trucks: Analysis of direct and indirect hybrid configurations. *Energy conversion and management*, 127:312–323, 2016.
- [33] Yoichi Shimoi and Yoshitaka Ono. Fuel cell system, September 27 2007. US Patent 2007/0224482 A1.
- [34] Rosa Elvira Silva, Fabien Harel, Samir Jemei, Raphaël Gouriveau, Daniel Hissel, Loïc Boulon, and Kodjo Agbossou. Proton exchange membrane fuel cell operation and degradation in short-circuit. *Fuel Cells*, 14(6):894–905, 2014.
- [35] J Solano, D Hissel, and M-C Pera. Modeling and parameter identification of ultracapacitors for hybrid electrical vehicles. In *Vehicle Power and Propulsion Conference (VPPC), 2013 IEEE*, pages 1–4. IEEE, 2013.
- [36] Phatiphat Thounthong, Viboon Chunkag, Panarit Sethakul, Bernard Davat, and Melika Hinaje. Comparative study of fuel-cell vehicle hybridization with battery or supercapacitor storage device. *IEEE transactions on vehicular technology*, 58(8):3892–3904, 2009.
- [37] Phatiphat Thounthong, Viboon Chunkag, Panarit Sethakul, Suwat Sikkabut, Serge Pierfederici, and Bernard Davat. Energy management of fuel cell/solar cell/supercapacitor hybrid power source. *Journal of power sources*, 196(1):313–324, 2011.
- [38] C. Turpin, D. Van Laethem, B. Morin, O. Rallières, X. Roboam, O. Verdu, and V. Chaudron. Modelling and analysis of an original direct hybridization of fuel cells and ultracapacitors. *Mathematics and Computers in Simulation*, 131:76–87, jan 2017.
- [39] Bouchra Wahdame, Laurent Girardot, Daniel Hissel, Fabien Harel, Xavier François, Denis Candusso, Marie Cecile Pera, and Laurent Dumercy. Impact of power converter current ripple on the durability of a fuel cell stack. In *Industrial Electronics, 2008. ISIE 2008. IEEE International Symposium on*, pages 1495–1500. IEEE, 2008.

- [40] Billy Wu, Michael A Parkes, Vladimir Yufit, Luca De Benedetti, Sven Veismann, Christian Wirsching, Felix Vesper, Ricardo F Martinez-Botas, Andrew J Marquis, Gregory J Offer, et al. Design and testing of a 9.5 kwe proton exchange membrane fuel cell–supercapacitor passive hybrid system. *international journal of hydrogen energy*, 39(15):7885–7896, 2014.
- [41] Qian Xun and Yujing Liu. Evaluation of fluctuating voltage topology with fuel cells and supercapacitors for automotive applications. *International Journal of Energy Research*, 43(9):4807–4819, 2019.
- [42] Qian Xun and Yujing Liu. Evaluation of fluctuating voltage topology with fuel cells and supercapacitors for automotive applications. *International Journal of Energy Research*, 43(9):4807–4819, jun 2019.
- [43] Qian Xun, Yujing Liu, and Elna Holmberg. A comparative study of fuel cell electric vehicles hybridization with battery or supercapacitor. In *2018 International Symposium on Power Electronics, Electrical Drives, Automation and Motion (SPEEDAM)*, pages 389–394. IEEE, 2018.
- [44] Qiao Zhang, Jiqiang Han, Gang Li, and Yan Liu. An adaptive energy management strategy for fuel cell/battery/supercapacitor hybrid energy storage systems of electric vehicles. *International Journal of Electrochemical Science*, 15(July):3410–3433, 2020.
- [45] Hengbing Zhao and Andrew F Burke. Fuel cell powered vehicles using supercapacitors—device characteristics, control strategies, and simulation results. *Fuel Cells*, 10(5):879–896, 2010.
- [46] Luis Zubieta and Richard Bonert. Characterization of double-layer capacitors for power electronics applications. *IEEE Transactions on industry applications*, 36(1):199–205, 2000.

Table 1: Electrochemical PEMFC model

Electrochemical model	Nomenclature
$E^{00} = \frac{-\Delta\bar{G}_f}{2F} = 1.32V$	(1) E^{00} Reversible cell voltage (V) $\Delta\bar{G}_f$ Gibbs free energy released F Faraday constant (s A/mol)
$\Delta E_P = A_{cd} \ln \frac{P_{SCH_2}}{P^0} + B_{cd} \ln \frac{P_{SCO_2}}{P^0}$	(2) ΔE_P E^{00} variation due to the pressure A_{cd}, B_{cd} Nerst potential coefficients P_{scx} Hydrogen/oxygen partial pressure at the catalytic sites (Pa) P^0 Standard pressure (Pa)
$\Delta E_T = \alpha + \beta T_{fc} + \gamma T_{fc}^2 + \delta T_{fc}^3 + v T_{fc} \ln T_{fc}$	(3) ΔE_T E^{00} variation due to the temperature $\alpha, \beta, \gamma, \delta, v$ Empirical coefficients T_{fc} Fuel cell temperature (K)
$E_N = E^{TP} = E^{00} - \Delta E_P - \Delta E_T$	(4) E_N Nerst potential
$\Delta V_{act} = AT_{fc} \ln \left(\frac{i_{fc} + I_n}{I_0} \right)$	(5) ΔV_{act} Activation over-voltage (V) I_n Internal current (A) I_0 Exchange current (A) A, B Over-voltage coefficients
$\Delta V_{conc} = BT_{fc} \ln \left(1 - \frac{i_{fc}}{I_l} \right)$	(6) ΔV_{conc} Concentration over-voltage (V) I_l Limit current (A)
$\Delta V_{ohm} = R_m i_{fc}$	(7) ΔV_{ohm} Ohmic losses (V) R_m Membrane resistance (Ω)
$V_m = (\Delta V_{act} + \Delta V_{conc} + \Delta V_{ohm}) + E_N$	(8) V_m Cell voltage (V)
$\frac{u_{fc}}{R_t} = NV_m$ with $i_{fc}(t) = C_{dl} \frac{dV_c(t)}{dt} + \frac{V_c(t)}{R_t}$	(9) N Number of cells $R_t C_{dl}$ Charge double layer effect V_c Dynamic part of the cell voltage (V)

Table 2: Thermal and fluidic PEMFC model

Thermal model model	Nomenclature	
$E^0 = \frac{\Delta h}{2F} = 1.48V$	(10)	E^0 Theoretical voltage close to the OCV
$\Delta S q_{EC} = \frac{N(E^0 - V_m) i_{fc}}{T_{fc}}$	(11)	$\Delta S q_{EC}$ Entropy flow due the exothermal electrochemical reaction (W/K)
$\Delta S q_{H_2} = 0$ and $\Delta S q_{O_2} = 0$	(12)	$\Delta S q_{H_2}, \Delta S q_{O_2}$ Entropy flow between the stack and the gas
$\sum \Delta S q = \Delta S q_{EC} + \Delta S q_{H_2} + \Delta S q_{O_2}$	(13)	$\Delta S q$ Entropy flow (W/K)
$T_{fc} = \frac{1}{C_{th}} \int (\sum \Delta S q - \Delta S q_{CW})$	(14)	C_{th} Thermal capacity of the stack (Ws/ K^2)
Fluidic model		
$P_x = P_{scx} + R_{dx1} q_x$	(15)	P_x Hydrogen/oxygen partial pressure at the fuel cell input (Pa) P_{scx} Hydrogen/oxygen partial pressure at the catalytic sites (Pa) R_{dx1} Pressure drop at the supply side (Pa s/ m^3) q_x Hydrogen/oxygen volume flow (m^3/s)
$q_{out} = \frac{P_{scx} - P_{sx}}{R_{dx2}}$	(16)	q_{out} Hydrogen/oxygen flow evacuated by the purge (m^3/s) P_{sx} Partial pressure at the anode/cathode side (Pa) R_{dx2} Pressure drop at the purge side (Pa s/ m^3)
$\frac{dP_{scx}}{dt} = \frac{1}{C_h} (q_x - q_{cx} - q_{xout})$	(17)	C_h Hydraulic capacitor q_x Hydrogen/oxygen volume flow (m^3/s) q_{cx} Hydrogen/oxygen volume flow consumed by the reaction (m^3/s) q_{xout} Hydrogen/oxygen volume flow consumed at the cell exhaust (m^3/s)

Table 3: Simulation model parameters

Fuel cell	500W, 15-32V, OCV=31.4V
Ultracapacitors	UC₁ = 8F 32V $u_{uc-init} = 30V$ $C2 = 1.0436 F$ $Ci1Veq = 0.1105 F/V$ $Ci0 = 5.4047 F$ $R2 = 4.3965 \Omega$ $Ri = 0.0428 \Omega$ UC₂ = 29F 32V $u_{uc-init} = 30V$ $C2 = 2.5192 F$ $Ci1Veq = 0.4821 F/V$ $Ci0 = 19.6415 F/V$ $R2 = 1.8933 \Omega$ $Ri = 0.0088 \Omega$ UC₃ = 58F 32V $u_{uc-init} = 30V$ $C2 = 4.35 F$ $Ci1Veq = 1.3579 F/V$ $Ci0 = 32.9676 F/V$ $R2 = 0.7738 \Omega$ $Ri = 0.0047 \Omega$
Diode resistance	2mΩ
Load power	300W
Hydrogen consumption cost	$N = 36$ cells $M_{H_2} = 2$ g/mol $F = 96485.3399$ As/mol $\lambda = 0.4$ $\dot{m}_{H_2-init} = 0$ $H2_{cost} = 0.0035$ US\$/gH ₂
FC degradation cost	$N_{switch} = 1$ $\delta_0 = 5 * 10^{-5}$ $\alpha = 4$ $p_{fc-nom} = 500W$ $FC_{cost} = 600$ US\$

Table 4: Objective function results

$C/cycle$	$C_{H_2}/cycle$	$C_{\Delta_{fc}}/cycle$	$C_{tot}/cycle$
29	0.00208	0.00410836	0.00610247
58	0.001867	0.00608777	0.008181

Table 5: Starting modes comparison - simulation

Mode	UC charge (s)	pre-time	FC max. current (A)	reached cur-	Number of FC turn on
Resistive	200		14.89		1
Short circuit	50		100		1
Progressive	50		100		1

Table 6: Starting modes comparison - validation

Mode	UC charge (s)	pre-time	FC max. current (A)	reached cur-	Number of FC turn on
Resistive	200		21.57		1
Short circuit	50		66		3
Progressive	50		66.29		3